Available online at www.sciencedirect.com

ScienceDirect

journal homepage: http://www.elsevier.com/locate/rpor

Original research article

The determination of a dose deposited in reference medium due to (p,n) reaction occurring during proton therapy

*Anna Dawidowska**, *Monika Paluch Ferszt*, *Adam Konefał*

Department of Nuclear Physics and Its Applications, Institute of Physics, University of Silesia, Katowice, Poland

ARTICLE INFO

Article history:
Received 31 August 2013
Received in revised form
15 November 2013
Accepted 27 February 2014

Keywords:
Neutrons
Proton therapy
Monte Carlo
GEANT4

ABSTRACT

Aim: The aim of the investigation was to determine the undesirable dose coming from neutrons produced in reactions (p,n) in irradiated tissues represented by water.
Background: Production of neutrons in the system of beam collimators and in irradiated tissues is the undesirable phenomenon related to the application of protons in radiotherapy. It makes that proton beams are contaminated by neutrons and patients receive the undesirable neutron dose.
Materials and methods: The investigation was based on the Monte Carlo simulations (GEANT4 code). The calculations were performed for five energies of protons: 50 MeV, 55 MeV, 60 MeV, 65 MeV and 75 MeV. The neutron doses were calculated on the basis of the neutron fluence and neutron energy spectra derived from simulations and by means of the neutron fluence–dose conversion coefficients taken from the ICRP dosimetry protocol no. 74 for the antero-posterior irradiation geometry.
Results: The obtained neutron doses are much less than the proton ones. They do not exceed 0.1%, 0.4%, 0.5%, 0.6% and 0.7% of the total dose at a given depth for the primary protons with energy of 50 MeV, 55 MeV, 60 MeV, 65 MeV and 70 MeV, respectively.
Conclusions: The neutron production takes place mainly along the central axis of the beam. The maximum neutron dose appears at about a half of the depth of the maximum proton dose (Bragg peak), i.e. in the volume of a healthy tissue. The doses of neutrons produced in the irradiated medium (water) are about two orders of magnitude less than the proton doses for the considered range of energy of protons.

* *Corresponding author*. Tel.: +48 510515756.
E-mail addresses: annadawidowska@gazeta.pl, a.dawidowska@us.edu.pl (A. Dawidowska).
http://dx.doi.org/10.1016/j.rpor.2014.02.003

1. Background

Cancer therapy using protons is a modern method of an external radiation treatment. It is characterized by high precision and efficiency.[1–6] Proton therapy differs from traditional methods of treatment in concentration of radiation dose in the tumor with a reduced load of healthy tissue in the input channel, precise placement of the dose in the target area with a large gradient at the border of healthy tissue and increased biological effectiveness. But this is not a universal method for the treatment of all types of pathological changes. The proton therapy is not used for spread tumors.

The undesirable phenomenon related to emission of protons is a production of neutrons in the system of beam collimators[7,8] and in irradiated tissues. The neutron production occurs in a broad range of proton energy. It causes proton beams to be contaminated by neutron radiation and patients to receive additional undesirable neutron dose. The presented research is associated with proton therapy in the range of relatively low energies from 50 MeV to 75 MeV. Such therapy is applied in a superficial tumor treatment, particularly in radiotherapy of ocular melanoma.[9]

2. Aim

The aim of the presented investigation was to determine the additional undesirable dose coming from neutrons produced in reactions (p,n) in an irradiated tissue represented by water – a medium recommended by dosimetry protocols for a dose determination in radiotherapy.[10] Water has the mass collision stopping powers and linear scattering powers approximately equal to those of biological tissues. The neutron doses were derived by means of the Monte Carlo computer simulations based on the GEANT4 software.

3. Materials and methods

The presented investigation was based on the Monte Carlo computer simulations with the use of the GEANT4 software in the version 4.9.3. The GEANT4 code is recommended by many scientists for application in proton and other kinds of radiotherapy[11,6,12–14] because it provides all physical processes occurring during the emission of proton therapeutic beams, based on extensive data bases of experimental parameters, cross-section, etc. The majority of physical process models is based on experimental data bases which makes it possible to obtain very accurate results. The calculations were performed for five energies of protons: 50 MeV, 55 MeV, 60 MeV, 65 MeV and 75 MeV applied in the proton therapy of the eyes.

The performed simulations made it possible to determine energy spectra, the map of fluence and the distributions of depth-doses for undesirable neutrons produced in the (p,n) reactions inside the irradiated volume, as well as the depth-dose distributions for the therapeutic protons. The created virtual simulated system consisted of a water phantom with logical detectors. The phantom was a cube of 5 cm × 5 cm × 5 cm. Two factors were taken into account for the choice of the size of a phantom. Firstly, the phantom of 5 cm × 5 cm × 5 cm is large enough not to disturb the flow of protons and neutrons. Secondly, the size used does not increase the time of simulations significantly. 201 logical detectors were located along the central axis of the proton beam (Z in Fig. 1). The logical detector system was shifted along the axis X, i.e. in the direction perpendicular to the proton beam central axis, to determine the maps of the neutron fluence. The logical detectors were in the shape of cylinders of 0.05 mm in height, the radius of its base being 5 mm. To obtain an accurate depth-dose distribution with the Bragg peak, the distances between the detectors were set as follows: 0.5 mm in the region of depths up to 3 cm, and 0.15 mm at 3–5 cm. A group of logical detectors was intended to the register of energies of neutrons. In this case, the distances between the

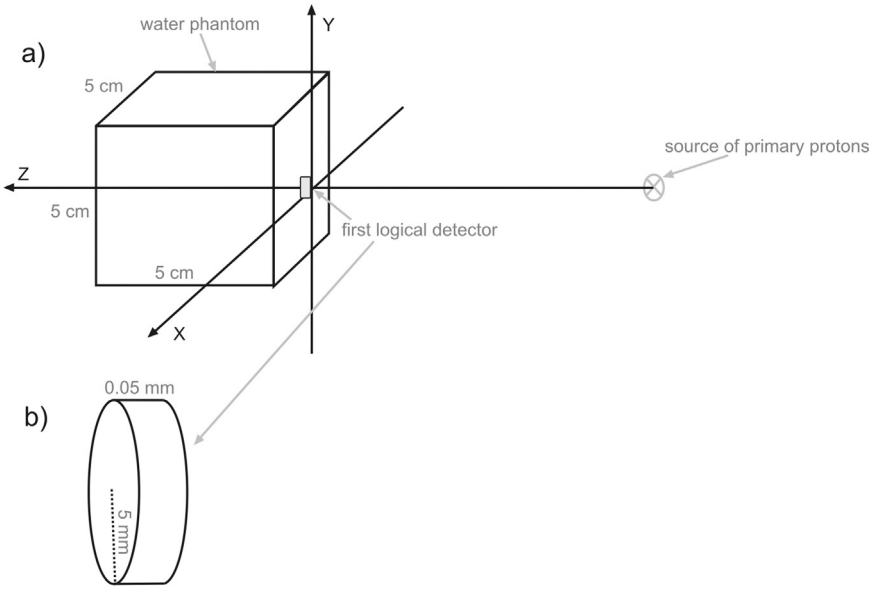

Fig. 1 – Scheme of the simulated system. (a) The full system and (b) a logical detector.

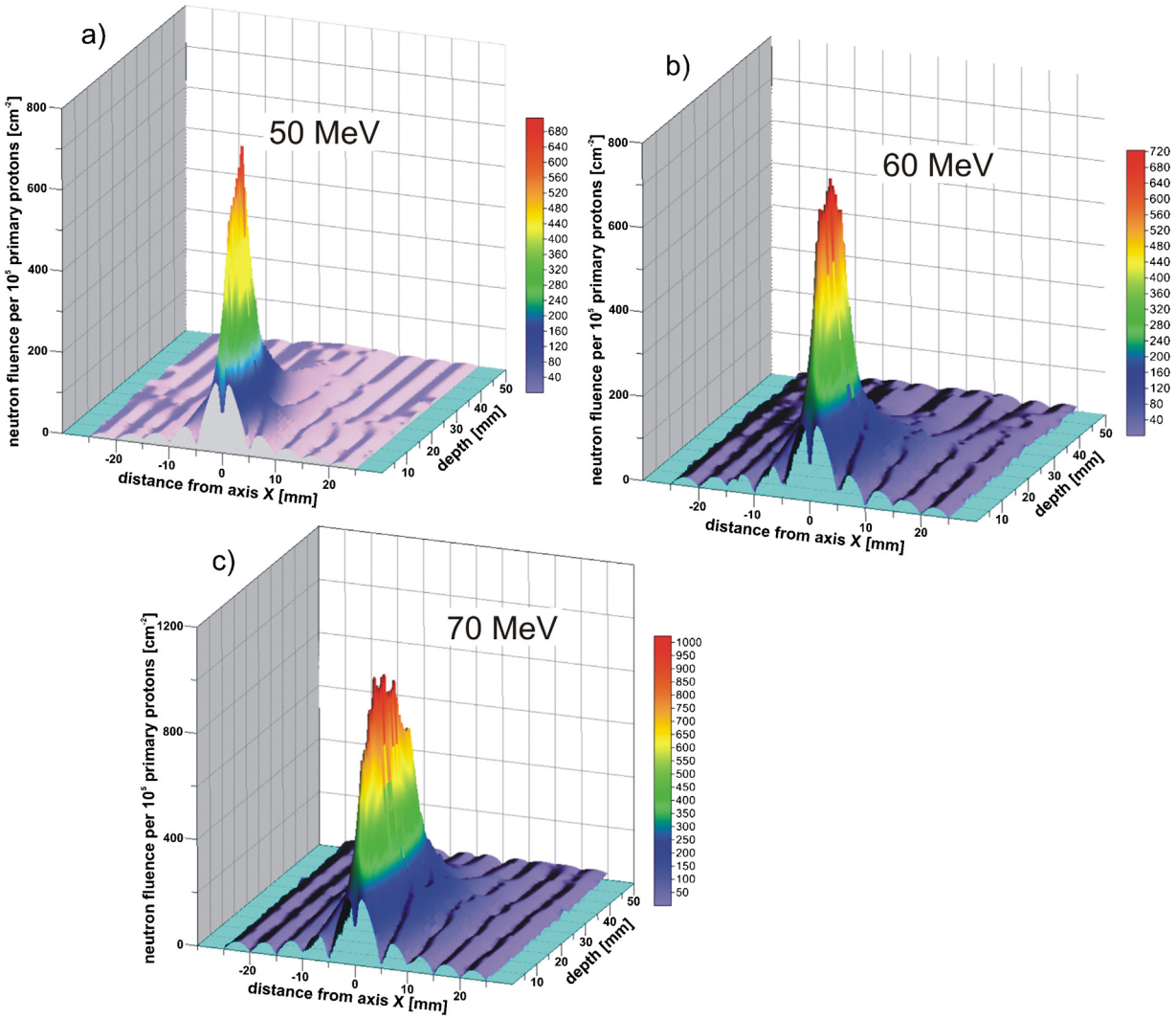

Fig. 2 – The maps of the neutron fluence for the chosen energies of the primary proton beams, (a) 50 MeV, (b) 60 MeV and (c) 70 MeV. The maps were obtained in the plane denoted by XZ in Fig. 1. The presented neutron fluence distributions are affected by statistical fluctuations.

detectors were equal to 1 mm. The proton source was located in vacuum (Fig. 1). The water phantom with a logical detector was surrounded by vacuum to avoid the neutron production outside the irradiated volume.

The primary proton beam was characterized by an energy spectrum and spatial distributions. In both cases, the Gauss distributions were used. FWHM of the energy spectrum was equal to 0.5 MeV, whereas it was 0.5 mm for the spatial distributions. We decided to consider the proton beam with the spatial distribution of 0.5 mm, because it is close to the clinical situation for the eye tumor therapy. Neutron doses were calculated on the basis of the neutron fluence and neutron energy spectra derived from simulations and by means of the neutron fluence–dose conversion coefficients taken from the dosimetry protocol of ICRP no. 74 for the antero-posterior irradiation (AP) geometry.[15] The neutron fluence–dose conversion coefficient is defined as an absorbed dose per unit neutron fluence in pGy cm^2. The values taken for the calculations were the averaged neutron fluence–dose conversion coefficients for superficial organs and tissues. These coefficients are the function of neutron energy. An average neutron energy registered in a logical detector was the basis of the choice of a suitable neutron fluence–dose conversion coefficient. The neutron doses can also be calculated by summing energy of neutrons deposited in the volume of a logical detector. However, such approach requires a much longer time for simulations or a larger computer power to obtain results with a relatively good statistic.

The simulations were carried out using computers in the Department of Nuclear Physics and Its Applications of the Institute of Physics of the University of Silesia in Katowice (Poland). The calculations were made on 3 GHz Pentium computers under the LINUX operation system.

4. Results

As mentioned before, the calculations were carried out for protons with five energies of 50 MeV, 55 MeV, 60 MeV, 65 MeV

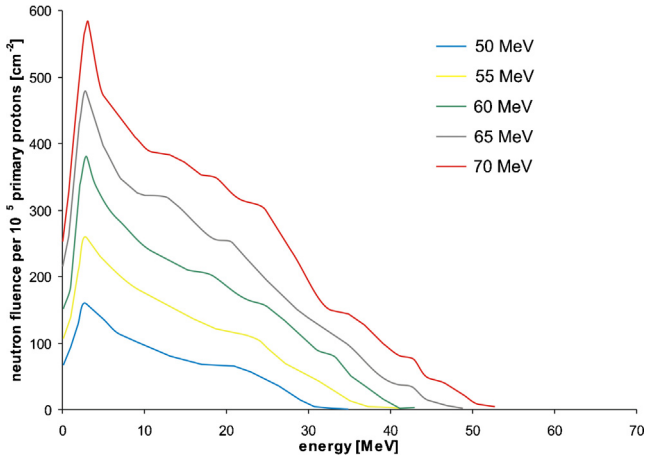

Fig. 3 – Neutron energy spectra for all considered energies of primary proton beams.

and 75 MeV. The obtained maps of the fluence of neutrons are presented in Fig. 2 (three-dimensional graphs), whereas the spectra of neutrons produced in (p,n) reactions in water are shown in Fig. 3. The maps were determined only in the plane *XZ* (see Fig. 1) because of the axial symmetry of the simulated system, i.e. the symmetry in relation to the central axis of the beam. The presented neutron fluence maps were obtained for 10^5 primary protons, whereas the neutron spectra were calculated for 2×10^6 primary protons to receive appropriately reduced uncertainties of the determined values.

The neutron fluence increases together with the increasing energy of protons. The most of the produced neutrons are registered along the proton beam at depths from 10 mm to 30 mm. The neutron fluence has its maximum located somewhat deeper for larger energies of the primary proton beam. The same tendency is visible for the width of the neutron fluence peak FWHM along the central axis of the proton beam, i.e. FWHM is equal to 10 mm, 12 mm, 14 mm, 18 mm and 23 mm for primary protons with 50 MeV, 55 MeV, 60 MeV, 65 MeV and 70 MeV, respectively.

The neutron spectra provided grounds for the calculations of neutron doses. Neutrons generated by the proton beams are characterized by broad energy spectra with the maximum of about 3 MeV (Fig. 3). The maximum energy of the produced neutrons increases with the increasing energy of the proton beam. It is equal to 35 MeV, 41 MeV, 45 MeV, 51 MeV and 59 MeV for the primary protons with energies of 50 MeV, 55 MeV, 60 MeV, 65 MeV and 70 MeV, respectively.

The neutron dose was determined for each logical detector. It makes it possible to present the neutron doses as a function of the depth in a water phantom. The neutron doses deposited in water are related to the neutron fluence values. Therefore, the largest neutron doses are located along the central axis of the proton beam. The neutron dose distributions along the central axis of the proton beam in water are presented in Fig. 4a. The neutron and proton doses for the chosen proton energy of 70 MeV are compared in Fig. 4b.

The neutron doses increase together with the increasing energy of primary protons (Fig. 5). Analogously to the neutron fluence distributions, the neutron doses have their maxima

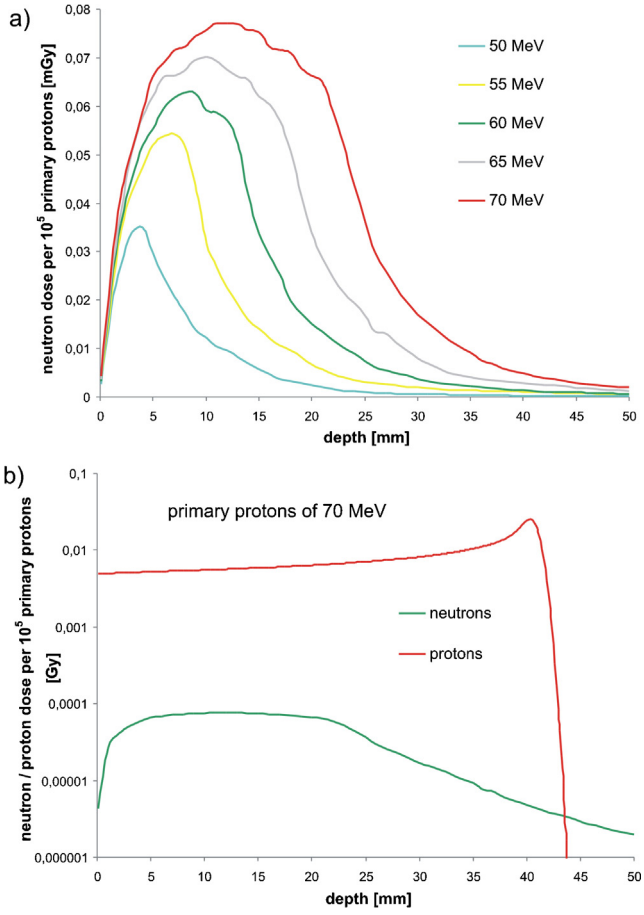

Fig. 4 – (a) The dependence between the neutron dose and the depth in water along the central axis of the proton beam for all considered energies. (b) The comparison between the neutron and proton dose distributions along the central axis of the proton beam with energy of 70 MeV in water.

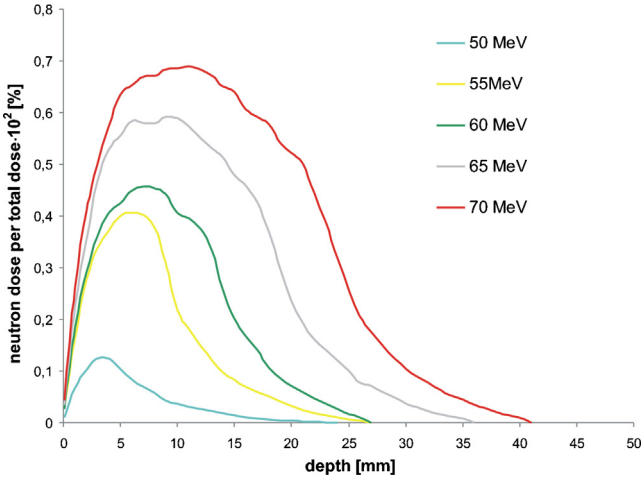

Fig. 5 – The percentage contribution of the neutron depth-dose to the total depth-dose along the central axis of the proton beam.

located deeper for larger energies of the primary proton beam. These maxima appear in the range of depths from 3 mm to 15 mm, depending on energy of the primary protons. The neutron dose at the Bragg peak depth is over one order of magnitude lower than at its maximum for all considered energies of the primary protons. In general, the neutron doses are much lower than the proton ones. They do not exceed 0.1%, 0.4%, 0.5%, 0.6% and 0.7% of the total dose at a given depth for the primary protons with energy of 50 MeV, 55 MeV, 60 MeV, 65 MeV and 70 MeV, respectively.

The small drops and gains visible in the curves in Figs. 4 and 5 are a result of statistical fluctuations.

5. Discussion

The use of the GEANT4 code ensures the high-quality results because this Monte Carlo toolkit is based on extensive data bases of parameters, cross-section, etc., adopted in the contemporary science.[16,17] In the presented study, the simulations of the inelastic scattering of protons were realized by means of the Binary Cascade model. This model generates the final state for hadron inelastic scattering by simulating the intra-nuclear cascade. The target nucleus is modeled by a three-dimensional collection of nucleons. The propagation through the nucleus of the incident proton and secondary particles is modeled by a cascading series of two-particle collisions occurring according to the particles' total interaction cross section. Between collisions, the protons and other produced hadrons are transported in the field of the nucleus by the Runge–Kutta method. Secondary particles are created during the decay of resonances formed during the collisions. The Binary model is based on the experimental data collected by the Particle Data Group and on parameterizations from the CERN-HERA collection. In the case of neutron interactions, the High-Precision model was implemented in the computer software. This model is composed of separate models for simulations of neutron capture, elastic scattering, fission, and inelastic scattering. The cross sections for the neutron processes are taken from the following data bases: Brond-2.1, CENDL2.2, EFF-3, ENDF/B-VI.0, ENDF/B-VI.1, ENDF/B-VI.5, FENDL/E2.0, JEF2.2, JENDL-FF, JENDL-3.1, JENDL-3.2 and MENDL-2.

As mentioned before, the neutron doses were calculated with the use of the neutron fluence–dose conversion coefficients taken from the dosimetry protocol of ICRP no. 74 for the antero-posterior irradiation geometry. Generally, these coefficients depend slightly on a chosen irradiated geometry. The AP geometry corresponds to the situation in which the ionizing radiation is incident on the front of the body in the direction orthogonal to the long axis of the body. Such situation appears in the case of neutrons induced by protons inside a patient. The produced neutrons travel through tissues approximately along the central axis of the proton beam which is usually incident on the front of the body perpendicular to the long axis of the body (for example the proton therapy of ocular melanoma).

In the presented study, water was the irradiated medium. This simplification is good enough for the calculations connected with the neutron production in the (p,n) reactions. Water has a density close to the soft tissues. Moreover, the (p,n) reactions in water as well as in the soft tissues occur mainly in interaction with nuclei of oxygen.

Doses of neutrons produced in water are accumulated mainly along the proton beam. They are about two orders of magnitude lower than the proton doses for the considered range of energy of protons. It is much less than the doses of neutrons produced in collimators of protons (several percent of the proton doses[18]). It is worth noticing that the therapeutic proton beam can be spread wider in the irradiated medium[19] (the situation not considered) and in such case the neutron dose can also be wider spatially distributed.

The maximum dose of neutrons induced by protons in water appears at about a half of the depth of the maximum proton dose corresponding to the Bragg peak. Thus, the region of the tissue with the maximum neutron dose is usually located in the volume of a healthy tissue. It is an unfavorable situation for a radiological protection of a patient.

It needs to be remembered that doses of neutrons produced in water increase with the increasing energy of protons. This increase is caused by an almost constant cross section for the inelastic nuclear proton reactions with nuclei of oxygen in the considered proton energy range (i.e. between 0.4 barn at 50 MeV and 0.3 barn at 70 MeV[20]). Moreover, the pion production occurs at the proton energies higher than the considered ones. Therefore, investigations connected with radiation produced in the irradiated patient are significant.

6. Conclusions

The investigation based on the Monte Carlo computer simulations indicates that:

- neutron production takes place mainly along the central axis of the beam where intensity of the proton beam is maximal,
- the maximum neutron dose appears at depths less than the Bragg peak, i.e. about a half of the depth of the maximum proton dose,
- greater neutron contributions to the total dose occur for greater energy of the proton beam,
- neutron depth-dose distributions are characterized by the growth at lower depths followed by a fall-off corresponding to the exponential curve,
- the determined neutron doses do not exceed 0.7% of the total dose,
- the determined neutron doses are in a good agreement with the experimental data presented by Moravek and Bogner[21] (the neutron doses lower than 1% of total dose).

Conflict of interest

None declared.

Financial disclosure

None declared.

REFERENCES

1. Hug EB, Fitzek MM, Liebsch NJ. Locally challenging osteo- and chondrogenic tumors of the axial skeleton: results of combined proton and photon radiation therapy using three-dimensional treatment planning. *Int J Radiat Oncol Biol Phys* 1995;**31**:467–76.
2. Kraft G. Tumor therapy with heavy charged particles. *Prog Part Nucl Phys* 2000;**45**:S473–544.
3. Miralbell R, Celia L, Weber D. Optimizing radiotherapy of orbital and paraorbital tumors: intensity-modulated X-ray beams vs. intensity modulated proton beams. *Int J Radiat Oncol Biol Phys* 2000;**47**:1111–9.
4. Brahme A. Recent advances in light ion radiation therapy. *Int J Radiat Oncol Biol Phys* 2004;**58**(2):603–16.
5. Paganetti H, Bortfeld T. Proton therapy. In: Schlegel W, Bortfeld T, Grosu AL, editors. *New technologies in radiation oncology*. New York: Springer; 2005. p. 345–63.
6. Cirrone GAP, Cuttone G, Mazzaglia SE, et al. Hadrontherapy: a Geant4-based tool for proton/ion-therapy studies. *Prog Nucl Sci Technol* 2011;**2**:207–12.
7. Shin D, Yoon M, Kwak J, et al. Secondary neutron doses for several beam configurations for proton therapy. *Int J Radiat Oncol Biol Phys* 2009;**74**:260–5.
8. Cywicka-Jakiel T, Stolarczyk L, Swakoń J, Olko P, Waligórski MPR. Individual patient shielding for a proton eye therapy facility. *Radiat Meas* 2010;**45**:1127–9.
9. Stolarczyk L, Olko P, Cywicka-Jakiel T, et al. Assessment of undesirable dose to eye-melanoma patients after proton radiotherapy. *Radiat Meas* 2010;**45**:1441–4.
10. IAEA TRS-398. *Absorbed dose determination in external beam radiotherapy: an international code of practice for dosimetry based on standards of absorbed dose to water*; 2000.
11. Titt U, Bednarz B, Paganetti H. Comparison of MCNPX and Geant4 proton energy deposition predictions for clinical use. *Phys Med Biol* 2012;**57**:6381–93.
12. Konefał A, Szaflik P, Zipper W. Influence of the energy spectrum and the spatial spread of the proton beams used in the eye tumor treatment on the depth-dose characteristics. *Nukleonika* 2010;**55**(3):313–6.
13. Tang S-B, Yin Z-J, Huang H, Cheng Y, Cheng F-H, Mao F-H. Geant4 used in medical physics and hadron therapy technique. *Nucl Sci Tech* 2006;**17**(5):276–9.
14. Sardaria D, Malekia R, Samavat H, Esmaeelia A. Measurement of depth-dose of linear accelerator and simulation by use of Geant4 computer code. *Rep Pract Oncol Radiother* 2010;**15**:64–8.
15. ICRP Publication 74. *Conversion coefficients for use in radiological protection against external radiation*; 1995.
16. http://www.geant4.web.cern.ch
17. Konefał A. Symulacje komputerowe metodą Monte Carlo przy pomocy nowoczesnego oprogramowania GEANT4. *Postępy Fizyki* 2006;**57**(6):242–51 [in Polish].
18. Cirrone GAP, private information.
19. Rajèan M, Pavloviè M. Track – a Monte Carlo computer code to assist design of scattering and collimating systems for proton therapy beams. *Rep Pract Oncol Radiother* 2004;**9**(6):235–41.
20. National Nuclear Data Center, Brookhaven National Laboratory, web retrieval system, http://www.nndc.bnl.gov/sigma/search.jsp
21. Morávek Z, Bogner L. Analysis of the physical interactions of therapeutic proton beams in water with the use of Geant4 Monte Carlo calculations. *Z Med Phys* 2009;**19**:174–81.